

# **DEVELOPMENT OF AN IMPEDANCE CARDIOGRAPH**

A dissertation  
submitted in partial fulfillment of the requirements for  
the degree of  
**Master of Technology**

by  
**Bharat A. Nihalani**  
(00307039)

Guide  
Prof. P. C. Pandey

Department of Electrical Engineering  
Indian Institute of Technology, Bombay  
January, 2002

INDIAN INSTITUTE OF TECHNOLOGY, BOMBAY  
DISSERTATION APPROVAL

Dissertation entitled: DEVELOPMENT OF AN IMPEDANCE CARDIOGRAPH

by **Bharat A. Nihalani**

is approved for the award of the degree of MASTER OF TECHNOLOGY

Supervisor ----- (Prof. P. C. Pandey)

Internal examiner ----- (Prof. Rakesh Lal)

External examiner ----- (Prof. L. R. Subramanyan)

Chairperson ----- (Prof. G. K. Sharma)

Date: 29<sup>th</sup> January, 2002.

# CONTENTS

Abstract	i
Acknowledgement	ii
List of abbreviations and symbols	iii
List of figures	iv
<b>Chapter/Section</b>	<b>Page no.</b>
<b>1 Introduction</b>	<b>1</b>
1.1 Overview	1
1.2 Project objective	1
1.3 Report outline	2
<b>2 Basics of impedance cardiography</b>	<b>3</b>
2.1 Introduction	3
2.2 Origin of impedance cardiogram	3
2.3 Modeling of thorax	4
2.3.1 Estimation of stroke volume, cardiac output and cardiac index	5
2.4 Impedance cardiography technique	8
2.5 Important considerations	9
2.5.1 Electrode system	9
2.5.2 Signal-to-motion artifact ratio versus frequency	9
2.6 Clinical applications	9
2.7 Limitations of ICG	10
<b>3 Testing of earlier hardware</b>	<b>11</b>
3.1 Introduction	11
3.2 Instrument description	11
3.2.1 ICG unit	11
3.2.2 Thorax simulator	12
3.3 Test results obtained from thorax simulator	13
3.4 Test results obtained with thorax simulator connected to the ICG unit	14

<b>4</b>	<b>Software developments</b>	<b>15</b>
4.1	Introduction	15
4.2	Signal acquisition	15
4.3	Signal processing	16
4.3.1	Overview of the offline signal processing program	16
4.3.2	Analysis of data from hardware with thorax simulator	16
4.3.2	Analysis of synthesized data	17
<b>5</b>	<b>Signal processing software test results</b>	<b>19</b>
5.1	Introduction	19
5.2	Test results with thorax simulator	19
5.3	Test results with synthetic data	19
<b>6</b>	<b>Summary and suggestions for future work</b>	<b>22</b>
6.1	Summary	22
6.2	Suggestions of future work	22
	<b>Figures</b>	<b>24-36</b>
	<b>Appendices</b>	
A	Earlier signal processing software	37
B	PCL-208 card settings	40
C	System specifications	41
	<b>References</b>	<b>43</b>

Bharat A. Nihalani / Prof. P. C. Pandey (Guide), "Development of an impedance cardiograph", *M.Tech. dissertation*, Department of Electrical Engineering, IIT Bombay, January 2002.

---

### **ABSTRACT**

Impedance cardiography (ICG) is the study of cardiac function determined from measurements of the electrical impedance of the thorax. It is an inexpensive, easy and non-invasive technique for determining stroke volume (SV) and cardiac output (CO).

The aim of this project is to develop an impedance cardiograph instrument. Towards this end, earlier hardware and software development carried out as part of M.Tech. projects at IIT Bombay have been used as the basis. In particular, the hardware developed by Babu Kuriakose in 1999 and software modules of Kedar Patwardhan in 1996 have been used. The hardware measures the signal providing thoracic impedance  $z(t)$ , its derivative  $dz/dt$ , base impedance of thorax  $Z_0$  and differentiated electrocardiogram  $d(\text{ECG})/dt$ . There is a thorax simulator as a separate unit to calibrate the impedance measurement unit. The analog signals from the hardware are acquired by a PC based data acquisition card. These signals are then fed to the offline signal processing program to get the heart rate (HR), stroke volume and cardiac output. Signal processing modules have been extremely tested using synthesized waveforms.

## ACKNOWLEDGEMENT

My primary thanks go to my guide *Prof. P.C.Pandey* for his invaluable guidance and immense help in giving me an insight into the project and also for availing me with the required text and laboratory facilities.

I would also like to thank my colleagues in the lab for their co-operation.

IIT Bombay  
January 2002

Bharat A. Nihalani  
(00307039)

## List of Abbreviations

Abbreviation	Term
AV	atrio-ventricular
CO	cardiac output
DAQ	data acquisition card
ECG	electrocardiogram
HR	heart rate
SV	stroke volume
CI	cardiac index
ICG	impedance cardiography
PC	personal computer
PCMCIA	personal computer memory card interface association
V/I	voltage-to-current
Pot	potentiometer
PCG	phonocardiogram

## List of symbols

Symbol	Explanation
L	length of the thorax under measurement
$Z_0$	basal impedance
$v$	changing volume
$\Delta V$	maximum change in volume
$\Delta Z$	maximum change in impedance
$Z_n$	impedance of changing volume
P	resistivity of blood
$T_{lvet}$	left ventricular ejection time
$z(t)$	instantaneous change in impedance
$(dz(t)/dt)_{max}$	maximum value of derivative of z w.r.t. time
$d(ECG)/dt$	derivative of ECG w.r.t. time

## List of figures

<b>Figure no.</b>		<b>Page no.</b>
Fig 2.1	Impedance cardiogram	24
Fig 2.2	Parallel column model	24
Fig 3.1	ICG system with the subject	25
Fig 3.2	ICG system with thorax simulator	25
Fig 3.3	Block schematic of ICG system	26
Fig 3.4	Block schematic of thorax simulator	26
Fig 3.5	Circuit diagram of thorax simulator	27
Fig 3.6	Circuit diagram of ICG system	28
Fig 4.1	Plot of acquired data ( $Z_o$ and $dz/dt$ ) with thorax simulator in ICG mode	29
Fig 4.2	Plot of acquired data ( $z$ and $dz/dt$ ) with thorax simulator in ICG mode	30
Fig 4.3	Plot obtained with thorax simulator in ECG mode	30
Fig 4.4	Plot of normal synthesized data	31
Fig 4.5	Plot of synthesized data with heart rate variation in step mode	31
Fig 4.6	Plot of synthesized data with heart rate variation in ramp mode	32
Fig 4.7	Plot of synthesized data with stroke volume variation in step mode	32
Fig 4.8	Plot of synthesized data with stroke volume variation in ramp mode	33
Fig 4.9	Plot of synthesized data with white gaussian noise	33
Fig 5.1	Result obtained with normal synthesized data	34
Fig 5.2	Result obtained with heart rate variation in step mode	34
Fig 5.3	Result obtained with heart rate variation in ramp mode	35
Fig 5.4	Result obtained with stroke volume variation in step mode	35
Fig 5.5	Result obtained with stroke volume variation in ramp mode	36
Fig 5.6	Result obtained with gaussian noise added synthesized data	36

# Chapter 1

## INTRODUCTION

### 1.1 Overview

Hemodynamic evaluation is an essential component in diagnosing cardiovascular disorders and managing patient care. There are numerous invasive, semi-invasive and non-invasive methods for evaluating hemodynamic function, which vary widely in the type of equipment, procedural complexity, cost and quality of data. Among these, ICG is a type of impedance plethysmography in which bioelectrical impedance is measured between electrodes positioned around the neck and around lower thorax. It is used primarily to calculate stroke volume and cardiac output, but it is also related to myocardial contractility, thoracic fluid content, and circulation to the extremities.

Impedance cardiography is based on the fact that blood is the most electrically conductive substance in the body. Blood volume and velocity change with each heart beat and result in a change in the electrical impedance of the chest. In order to measure this impedance change, generally a four-electrode scheme is used. Here, two outer electrodes inject a high frequency current in the thorax and the two inner electrodes sense the voltage modulated by the thoracic impedance. The variation in the impedance as a function of time is used, with the thoracic impedance models, for estimating the stroke volume, i.e. the amount of blood pumped with each heart beat and for obtaining related diagnostic information.

### 1.2 Project Objective

As part of the ongoing work for development of system for impedance cardiography at IIT Bombay, Babu Kuriakose has earlier developed, as his M.Tech. project [1], the hardware for an impedance cardiograph and a thorax simulator. In this project, the hardware developed earlier has been fully tested, block-by-block, and as a unit. Software for signal acquisition using a PC based A/D card, processing and display has been developed by making use of the program developed earlier by Kedar Patwardhan as part of his M.Tech. project [2]. The signal processing modules have been tested by using appropriate simulated waveforms. Finally, the hardware and software part have been used together.

### **1.3 Report Outline**

The second chapter describes the basic fundamentals of impedance cardiography. Origin of the impedance waveform is discussed followed by thorax modeling considerations. Finally, the basic technique of thoracic impedance measurement and its applications are mentioned.

Chapter 3 gives a detailed description of the earlier developed hardware followed by results obtained by testing the various blocks of the hardware unit.

Chapter 4 describes the software developed earlier and is followed by the further developments achieved in terms of signal acquisition and processing. The results obtained from the signal processing algorithm for various types of data are explained in the fifth chapter. The last chapter provides a summary of the work done and conclusions.

Appendix A explains the offline implementation of the signal processing algorithm developed by Kedar Patwardhan. Appendix B lists the settings for the PCL-208 data acquisition card. Appendix C gives the system specifications.

## Chapter 2

### BASICS OF IMPEDANCE CARDIOGRAPHY

#### 2.1 Introduction

Biological materials such as bone, muscle, blood, urine etc. are poor conductors of electricity, relative to conductors but their conductivity is better as compared to that of insulators. Resistance measurement becomes difficult in biological materials or any electrolytic substance as the application of steady electric field results in polarization at electrodes. The factors responsible for such polarization are:

- a) the capacitance formed by the electrodes with biological specimen as the dielectric and
- b) the capacitance effect of the double layer at the surface of the electrodes.

This difficulty is reduced to a large extent by employing sinusoidal electric field in place of DC current. The quantity measured using sinusoidal field is referred to as impedance ( $Z$ ), in place of resistance, due to the frequency dependent character of the former. The frequency of the time varying field is normally chosen between 10 kHz and 400 kHz [3] for measurement on biological materials as the effects described above are reduced to a large extent.

As its name implies, impedance cardiography measures the total impedance, or resistance to the flow of electricity, in the chest. Impedance is represented by the symbol  $Z$  and is measured in ohms. Average thoracic impedance, or  $Z_0$ , is also known as the base impedance and reflects the total fluid status of the chest, since blood is a better conductor of electricity as compared to other tissue. Electrical current travels more easily through a chest in which plasma and fluid have accumulated due to pulmonary edema, effusions, or infiltrates, so the reduced impedance is reflected in a low  $Z_0$  value.

#### 2.2 Origin of impedance cardiogram

The thorax is the part of the body between the neck and the abdomen. It mainly comprises of the heart and the lungs. Due to simultaneous blood volume changes taking place in different compartments of the thoracic cavity, the impedance of the thorax changes. This change may be, for example, due to simultaneous contraction of both the ventricles and subsequent rapid ejection of blood that produces a decrease in

ventricular blood volume, whereas an increase in blood volume in the aorta, pulmonary arteries and pulmonary capillaries.

It has been found [4] that the regions most likely responsible for impedance change, namely atria, lungs and aorta, receive only a fraction of the stroke volume (SV). Hence, it appears that the blood volume movement in the aorta and the great veins mainly contributes the impedance cardiogram. The change in impedance is obtained due to blood volume changes in the aorta during one cardiac cycle and the alignment of erythrocytes (red blood cells).

During systole, the erythrocytes get aligned due to increased volume and velocity of blood in the aorta that lowers impedance. During diastole, erythrocytes get randomly aligned due to less volume and velocity of blood in the aorta that increases impedance.

Referring to the impedance waveform, Fig 2.1 shows  $-\Delta Z$  plotted along with  $dz/dt$  in synchronism with the ECG waveform. Figure shows points B and X, which denote the aortic valve opening and closure, respectively. The time interval between the points B and X reflects the ventricular ejection time. The C point ( $dz/dt_{\max}$ ) corresponds to the maximum impedance change. An A wave precedes the opening of the aortic valve and corresponds to atrial filling (atrial diastole). An O wave, which has a relationship with mitral valve closure, represents the rapid ventricular diastole. This wave may be used to identify patients at higher risk for various forms of cardiomyopathies and also for predicting outcomes in terms of disability and death. A pronounced O wave was found in patients with mitral regurgitations. The  $dz/dt$  waveform provides a significant amount of diagnostic information [4]. Impedance cardiogram is the variation in the value of the instantaneous impedance from the base impedance of thorax.

### **2.3 Modeling of thorax**

Since the last few decades, attempts have been made to model the thorax with the help of electrical models. Simplified lumped parameter models were used as compared to the more complex models based on predicting changes in current density distribution accompanying physiological activity, and resulting electrical fields. In order to model a particular body segment, it was approximated electrically by a cylinder of bone surrounded by muscle, with cylindrical blood vessels parallel to the bone distributed within the muscle. Such a combination then suggested three structures in parallel,

each having a value of R determined by its resistivity and its ratio of L/A. The lower resistivity values of blood and muscle relative to bone indicated that these two components dominated in determining the resulting resistance of the body segment.

The technique of ICG was first introduced by Nyboer et al (1940) [3] who later proposed the “parallel conductor theory” for the estimation of stroke volume in 1960. His theory modeled the action of systole to place additional impedance  $Z_b$  in parallel with the base impedance of the body segment  $Z_o$  at the end diastole.

Later, in 1966, Patterson and Kubicek [4] developed this technique further for impedance measurement and assumed that the lungs, which receive the output of the right ventricle during the systole, were the source of the impedance change. The model used to quantify the impedance changes is known as the parallel column model, as shown in Fig 2.2 [4]. In this model, the basal impedance of thorax is represented by a column M of conducting material with constant impedance  $Z_o$  and a parallel column N of varying volume representing the lungs whose volume and hence impedance change during each heartbeat.

### 2.3.1 Estimation of Stroke Volume, Cardiac Output and Cardiac Index [1]

The net impedance in the parallel model of Fig 2.2 is given as

$$Z = Z_o \parallel Z_n \quad (1)$$

As the area of column N changes from zero to a final value, there is a small change in impedance across the columns given as

$$\begin{aligned} z &= Z - Z_o \\ &= -\frac{Z_o^2}{Z_o + Z_n} \end{aligned} \quad (2)$$

Assuming that  $Z_n \gg Z_o$ ,

$$z = -\frac{Z_o^2}{Z_n} \quad (3)$$

The impedance of column N, with cross section area A, length L and volume  $v = LA$ , is given as

$$\begin{aligned} Z_n &= \frac{\rho L}{A} \\ &= \frac{\rho L}{(v/L)} \\ &= \frac{\rho L^2}{v} \end{aligned}$$

Substituting it in equation (3), we get,

$$z = -\frac{Z_o^2}{\rho L^2} v$$

Thus, the instantaneous value of the change in thoracic impedance is related to change in blood volume, i.e.

$$Z(t) = -\frac{Z_o^2}{\rho L^2} v(t)$$

Since  $Z(t)$  is very small,  $Z_o$  can be taken as the base impedance ,

$$Z_o \cong \text{avg}[Z(t)] \quad (4)$$

Here the assumption is that during systole, the inflow of blood into the lungs is the source of impedance change. Under this assumption, the blood volume  $\Delta V$  is the stroke volume and can be related to maximum change in impedance  $\Delta Z$  as

$$\begin{aligned} \Delta Z &= (-z(t))_{\max} \\ \Delta V &= \rho \frac{L^2}{Z_o^2} \Delta Z \end{aligned}$$

Above equation relates the impedance change to the net blood volume change and assumes that the lungs were the source of the impedance change.

The volume of the small parallel column is zero just before systole. During systole, the volume of lungs increase with the inflow of blood and this change is modeled by an increase in cross sectional area of the parallel column. To consider the blood that leaves the lungs during systole, a forward slope extrapolation procedure is used as shown in the Fig 2.1. Drawing the slope by forward extrapolation has been replaced by the use of the first derivative of the impedance change. The extrapolation of  $\Delta Z$  is obtained by using the product of the negative peak (minimum) of  $dz/dt$  (shown upward on the graph) and the left ventricular ejection time, which is determined from the last upward crossing of  $dZ/dt$  before the large systole peak to the second heart sound. The formula for stroke volume thus gets modified as

$$\Delta V = \frac{\rho L^2}{Z_o^2} \left( -\frac{dz}{dt} \right)_{\max} T_{lvet} \quad (5)$$

where,

$(dz/dt)_{\min}$  = the most negative deflection during systole measured from zero.

$T_{lvet}$  = ventricular ejection time.

$\rho$  = resistivity of blood, normally taken to be 150  $\Omega\text{cm}$ .

For higher accuracy haematocrit percentage based correction to  $\rho$  may be applied and replaced by the product of S and  $\rho_n$  [12], where

$$S = 2.624 - 1.121 \log_{10} HCT \quad \text{and}$$

$$S = 68 \exp(0.025 HCT)$$

Cardiac output is computed by multiplying the stroke volume value by heart rate.

The perfusion significant blood flow - the cardiac index, CI, is then calculated as

$$CI = \frac{CO}{BSA}$$

where, BSA – estimated value of the surface area of the body expressed in square meters [12].

## **2.4 Impedance Cardiography Technique**

The basic technique of measuring transthoracic impedance employed in most of the presently developed systems includes injection of a high frequency (10 kHz-400 kHz) low amplitude current (2-4 mA) through skin electrodes and measuring the voltage variation according to the impedance change  $z(t)$ .

A typical impedance measuring system is comprised of a sine-wave oscillator followed by a voltage to current converter. The constant current output of the converter is passed through the thorax region by a pair of current electrodes. Voltage signal developed along the current path is sensed with the help of another pair of electrodes. Because of variation in the thoracic impedance, the voltage signal is an amplitude modulated signal with the current excitation frequency as the carrier and the impedance variation as the envelope. The voltage signal thus obtained is amplified and detected to obtain a signal that is proportional to instantaneous impedance of the thorax.

## **2.5 Important Considerations**

### **2.5.1 Electrode system**

The ICG system originally developed by Kubicek et al [3] used two sets of circumferential band electrodes. A current of 100 kHz, 4 mA was fed into a pair of electrodes (E1 and E4) and the voltage was picked up by another pair of electrodes (E2 and E3). Many studies have been made on the use of spot electrodes in place the band electrodes. It was found that the use of band electrodes involved less distortion [5]. Patterson [4] performed experiments with electrodes in different regions for the supine and sitting positions and found that spot electrodes present large errors. But there are problems associated with the use of band electrodes as compared to spot electrodes, such as the problems of motion artifacts and polarization. Use of band electrodes may be objectionable in certain areas such as the neck and the abdomen. Combination types of electrodes with band electrodes for current and spot electrodes for voltage on sides of chest have also been proposed [3].

### **2.5.2 Signal-to-motion artifact ratio versus frequency**

A major problem in the measurement of transthoracic impedance is the presence of motion artifacts. Expect for the change in transthoracic impedance due to change in

volume of lungs during ventricular systole, there are possible sources, such as changes in electrode position, skin-electrode impedance or diaphragm movement.

Studies have shown that measured change in impedance increases with increasing frequency [6]. The skin-electrode impedance is high at frequencies below 10 kHz, and therefore it swamps the variation. Hence frequencies above 10 kHz should be used. Frequencies above 400 kHz are not desirable because of possible radio frequency interference and artifacts arising from the coupling of subject to ground. Therefore, commercial equipments operate at a single frequency between 10 kHz and 400 kHz.

## **2.6 Clinical Applications**

Noninvasive cardiac output monitoring with ICG helps in outpatient management of congestive heart failure patients, in the pacemaker clinic for pacemaker optimization, and in diagnosing early rejection in heart transplant patients. This technique is clinically employed [4] for various conditions such as cardiac valvular diseases, deep vein thrombosis, ischemic heart diseases, peripheral vascular occlusive disease etc. In addition to these, this technique can be used for continuous monitoring of stroke volume and cardiac output non-invasively in intensive care units.

## **2.7 Limitations of ICG**

Although ICG monitoring offers a wide range of applications, it is limited in patients immediately following sternotomy, those with excessive movement, those with tachycardia greater than 250 beats per minute and those with aortic valve regurgitation [7]. Although ICG has been utilized in all of these instances, accuracy of data may be affected due to changes in the thorax models considered during measurement that introduce uncertainties in the relationship between the impedance change and stroke volume. The flow pattern and magnitude in the aorta or vena cavae vary from person to person resulting in different contributions to  $\Delta Z$  by the blood resistivity variations in the various vessels.

Extremely large amounts of thoracic fluid may interfere with the impedance signal, making hemodynamic data unattainable or unreliable. Conditions such as severe pulmonary edema may decrease the signal-to-noise ratio, damp the  $dz/dt$  waveform, and inhibit hemodynamic data acquisition. However,  $Z_0$ , the primary ICG measurement, can always be obtained and displayed. As the extreme volumes of

thoracic fluid decrease, the signal-to-noise ratio improves and hemodynamic data becomes available.

## **Chapter 3**

### **TESTING OF EARLIER HARDWARE**

#### **3.1 Introduction**

This chapter gives a block-by-block description of the hardware as developed by Babu Kuriakose [1] and the results obtained by testing the various blocks. The present unit involves an ICG instrument that captures the impedance variations of the thorax and carries out further processing to obtain the following signals, namely impedance  $z(t)$ , its derivative  $dz/dt$ , base impedance  $Z_0$  and  $d(\text{ECG})/dt$ . A thorax impedance simulator used for testing and calibration of the instrument is also implemented. A brief explanation of the overall instrument is given below followed by the test results obtained.

#### **3.2 Instrument description**

The overall unit consists of two separate blocks, namely the ICG extraction unit and the thorax simulator unit. The ICG unit can either be connected to the patient to capture impedance and ECG signals as shown in Fig 3.1 or to the thorax simulator unit for testing and calibration of the ICG unit as shown in Fig 3.2.

Referring to the above mentioned figures, I1 and I2 are the current injecting electrodes and V1 and V2 are the voltage sensing electrodes. The various sub blocks of the ICG system are explained below.

##### **3.2.1 ICG unit**

The ICG system consists of various sub blocks as shown in Fig 3.3.

##### **1) Current excitation**

This block is used for injecting a high frequency current to the subject's thorax. A Wein-bridge oscillator circuit is used to generate a stable high frequency sinusoidal signal whose output is fed to a voltage-to-current converter circuit to provide a current source excitation. The excitation current is injected to the subject through a pair of suction cup electrodes. For voltage sensing, another pair of suction cup electrodes is used. The signal is then fed to an ICG extraction circuit for signal conditioning.

## 2) ICG extraction

ICG extraction circuit gives  $z(t)$ ,  $dz/dt$ ,  $Z_0$  and  $d(\text{ECG})/dt$  signals. The front end of this unit is an instrumentation amplifier with 16 kHz high pass filter at the input. It is used for eliminating the power line interference, ECG and other motion artifacts. To demodulate the signal a full wave precision rectifier followed by a first order lowpass filter with cutoff frequency of 0.72 Hz is used. The filtered signal consists of basal impedance  $Z_0$ , changing impedance  $z(t)$  signal and large amount of respiration components that are subsequently removed by a DC cancellation circuit. Then impedance signal is amplified and fed to a differentiator having a corner frequency of 50 Hz. The output of differentiator gives the  $dz/dt$  signal.

## 3) ECG extraction

Another instrumentation amplifier amplifies the ECG signal. It has a low pass filter having a corner frequency of 40 Hz and removes all 100 kHz carrier components from the ECG signal. In order to reduce the effect of large artifacts at low frequency, a first order high pass filter with corner frequency of around 0.2 Hz is used. The signal is differentiated using a differentiator with a corner frequency of 12 Hz to get  $d(\text{ECG})/dt$  signal. It is advantageous to use a right leg electrode connected to circuit ground, in order to reduce dc offset errors and common mode pick-up. This electrode should have a protection resistance in series with it.

## 4) Power supply requirements

ICG instrument and thorax simulator circuits use separate power supplies. ICG instrument is driven from a  $\pm 12$  V, 110 mA dual supply.

### 3.2.2 Thorax simulator

In order to verify the proper operation of the ECG and ICG circuits, this block is implemented as a separate hardware block. It simulates

1. Thorax impedance consisting of a fixed impedance  $Z_0$  and varying impedance  $z(t)$ .
2. ECG signal with common mode and differential mode components.
3. Tissue-electrode contact resistance.

The block schematic of the thorax simulator is as shown in Fig 3.4. The basic unit consists of an astable multivibrator to generate voltage waveforms for the impedance

simulator whose frequency can be varied by a potentiometer provided on the board. For impedance variation, an analog switch is used, controlled on/off by the control signal obtained from the astable multivibrator. With astable multivibrator circuit both impedance and ECG waveforms can be simulated, one at a time with the help of a SPDT switch. Another switch is used to select ECG either in common mode or differential mode. The amount of common mode and differential mode signal can be controlled by two potentiometers e1 and e2.

Thorax simulator circuit uses a 9 V battery, which converts into a split power using op-amp circuit.

### 3.3 Test results obtained from thorax simulator

As mentioned in the previous section, the thorax simulator is used to simulate the impedance and ECG signals. The circuit diagram implementation of the thorax simulator is as shown in the Fig 3.5.

The time control potentiometer of the simulator was adjusted to have 1 Hz square wave. ECG signal can be measured in the common mode and difference mode.

In the common mode, the following voltages were obtained at V1 and V2.

Position of pots e1 and e2	V1 (p-p)	V2 (p-p)
Leftmost	140 mV	140 mV
Rightmost	7 mV	7 mV

Here, the waveforms at V1 and V2 were in phase with each other. In the differential mode, the following voltages were obtained at V1 and V2 for the leftmost position of pots e1 and e2.

$$V1 (p-p) = 8 \text{ mV}$$

$$V2 (p-p) = 20 \text{ mV}$$

Here, the waveforms at V1 and V2 were in phase opposition with each other. The results obtained for ECG in the two modes are summarized in the table below.

Mode	$V_{cm} (p-p) = (V1+V2)/2$	$V_{dm} (p-p) = V1 - V2$
Common mode	140 mV	< 2 mV
Differential mode	6 mV	30 mV

### 3.4 Test results obtained with thorax simulator connected to the ICG unit

In order to test the performance of the ICG unit, the thorax simulator was connected to it through four independent shielded cables. The current injected by the ICG unit was 3.3 mA rms at 100 kHz. In order to obtain the impedance signal, the ICG mode in the thorax simulator is selected and the time control potentiometer is set at 1 Hz. Referring to the circuit diagram of the ICG unit in Fig 3.6, the output obtained at various points are given below.

$$V_9 = 1.8 V_{p-p} \text{ output of ICG instrumentation amplifier.}$$

$$V_{10} = 60 \text{ mV}_{p-p} \text{ square wave superimposed on } 5.6 \text{ V dc } [Z(t)]$$

$$V_{11} = 6.2 \text{ V dc } [Z_0]$$

$$V_{12} = 600 \text{ mV}_{p-p} \text{ square wave superimposed on } -100 \text{ mV dc}$$

$$V_{13} = 2.24 V_{p-p} \text{ square wave superimposed on } -500 \text{ mV dc } [z(t)]$$

$$V_{14} = 18 V_{p-p} \text{ square wave } [dz/dt]$$

The gain of the  $z(t)$  amplifier can be adjusted by potentiometer  $R_{35}$ . Hence, the ac part of  $V_{13}$  could vary from 2 V to 4 V.

## Chapter 4

### SOFTWARE DEVELOPMENTS

#### 4.1 Introduction

There have been several student projects towards the development of an impedance cardiograph system since 1990 at IIT Bombay [1][2].

As regards the software development, in 1996, Kedar Patwardhan [2] modified the program for offline signal processing and display earlier developed by Joshi. He also developed programs to acquire signals using the PC with ISA bus based data acquisition card, a notebook PC with PCMCIA based data acquisition card, and a compact data logger with multi-channel analog inputs.

This chapter describes modifications and developments in software achieved as a part of this project. The present work involved developing a package for signal acquisition and various offline signal processing and analysis programs. Towards this end, the various modules developed earlier by Patwardhan have been used wherever appropriate.

#### 4.2 Signal acquisition

Signal acquisition is carried out with the help of PCL-208 (DMS) data acquisition card. Kedar Patwardhan had earlier developed software for signal acquisition and processing. His program continuously digitized the impedance signal  $z(t)$ , its derivative  $dz/dt$ , ECG  $e(t)$  and optionally PCG waveforms, stored them into binary files and processed them to estimate the value of HR, SV and hence CO. The waveforms were sampled at a fixed sampling frequency of 200 Hz. In the modified approach, a program ICG\_ACQ has been developed in which the  $z(t)$ ,  $dz/dt$  and  $e(t)$  waveforms are continuously recorded and stored into binary files. There is no processing carried out during signal acquisition. PCG signal may be optionally sampled along with the other signals. The PCG signal is sampled only once and 10,000 sample points are acquired and stored in a binary file with (.PCG) extension. The acquired data are further processed and analyzed by the offline processing program developed by Kedar Patwardhan. The sampling frequency can be varied as desired from 100 Hz upto 3,000 Hz. Two thousand samples of each of the three signals are acquired, hence the time of acquisition may vary from 20 secs to 0.67 sec.

The reason for choosing 2,000 sample points was that the offline processing program was designed for 2,000 sample points of each signal. The sampling frequency of the PCG signal is thrice the sampling frequency of the other three signals. Data transfer to the PC bus takes place by polling the EOC as opposed to the interrupt based data transfer used in the earlier approach.

### **4.3 Signal processing**

This section gives an overview of the offline signal processing algorithm implementation developed earlier by Patwardhan [2] and is followed by analysis of this program for data from the hardware with thorax simulator and for synthesized data with and without the presence of noise. A more detailed description of the algorithm implementation is given in the Appendix A.

#### **4.3.1 Overview of the offline signal processing program**

The program for offline signal processing and display is SPA2B. An enhanced version for detecting QRS complex locations in the ECG has been used. Using these locations as the reference mark, the  $dz/dt$  signal is ensemble averaged. From this LVET and  $(dz/dt)_{\min}$  are found. Base impedance is found by averaging  $z(t)$ . Stroke volume is calculated using the equation derived by Kubicek. Heart rate is found from QRS complex intervals, and this, along with stroke volume for calculating cardiac output. A provision to view zoomed version of the waveforms and to process them cyclewise is also added.

#### **4.3.2 Analysis of data from the hardware with thorax simulator**

The thorax simulator is used to simulate the impedance and ECG signals and is connected with the ICG signal extraction unit. The ICG signal extraction block gives four signals at the output, namely  $Z_o$ ,  $z(t)$ ,  $dz/dt$  and  $d(ECG)/dt$  waveforms. With the thorax simulator connected to it, at any instant of time, either impedance or ECG signal can be obtained. This choice can be made with a SPDT switch provided on the thorax simulator block. When the impedance mode of signal is selected, the  $Z_o$ ,  $z(t)$  and the  $dz/dt$  waveforms are available at the output and the ECG signal is zero, while in the ECG mode, only ECG signal is available at the output. Signals in these two modes are acquired and stored by the signal acquisition program ICG\_ACQ. A plot of the acquired signals in both the modes is as shown in figures Fig 4.1, Fig 4.2 and Fig

4.3. The first plot shows the  $Z_o$  along with  $dz/dt$  signals. The impedance variations that can be seen around the  $Z_o$  point are amplified to obtain the  $z(t)$  signal which is shown in the Fig 4.2 along with the  $dz/dt$  signal. Finally, a plot of the ECG signal is shown in Fig 4.3. These plots obtained are with frequency of heart rate set at 0.8 Hz for the first two plots and 1 Hz for the third. This can be varied by a pot provided on the thorax simulator from 0.5 Hz to 4.4 Hz in order to simulate the variations in the heart rate. But the waveshape of impedance and ECG waveforms obtained at the output of the hardware unit are different when compared with the standard published waveforms. Hence, when these signals are fed to the offline analysis program, meaningful results are not obtained.

#### **4.3.3 Analysis of synthesized data**

The synthesized data are taken from the published waveforms. A plot of one such set of data is shown in Fig 4.4. It shows the impedance, ECG and PCG waveforms. This data is written into a binary file and fed to the offline processing program SPA2B. The synthesized data are modified in order to simulate changes in heart rate and stroke volume as explained below.

a) Heart rate variation: In order to simulate variations in heart rate during exercise or various cardiovascular diseases, a program ICG\_SIMU was developed. In this program, heart rate is varied in a specific range as specified by the user during program execution by altering the ECG signal along with the  $dz/dt$  signal. The basic technique is to insert certain number of zeros between two successive cycles. The variation may be done in two modes, namely step mode and ramp mode. In the step mode, heart rate takes only two values; ECG data represents one value of heart rate for the first half of the sample points and represents another value for the second half as shown in Fig 4.5. In the ramp mode, the heart rate varies in a linear fashion from one value of heart rate to another as shown in Fig 4.6.

b) Stroke volume variation: In the next case, only variation in stroke volume is simulated by a program SV\_SIMU keeping the heart rate constant. This is achieved by scaling the  $dz/dt$  signal. In this program, stroke volume varies between two values either in step mode or ramp mode. In the step mode, the  $dz/dt$  signal is scaled to a particular value for the first half of sample points and to another value for the second half as shown in the Fig 4.7. In the ramp mode, the stroke volume is varied in a linear fashion between the range specified by the user as shown in the Fig 4.8.

c) Finally, the synthetic data are added with white gaussian noise for varying SNRs in order to check the robustness of the signal processing algorithm. The program SNR\_DB adds white gaussian noise to the input data file with the specified SNR. A plot of synthetic data in the presence of noise is shown in the Fig 4.9. The results obtained are described in the next chapter.

## Chapter 5

### SIGNAL PROCESSING SOFTWARE TEST RESULTS

#### 5.1 Introduction

This chapter deals with the results obtained from the signal processing algorithm as applied on the data acquired from the hardware with thorax simulator and synthetic data. The results are obtained in terms of the various physiological parameters ( $Z_o$ , HR,  $T_{lvet}$ , SV, CO). The display obtained as output of the offline processing program is shown for the different cases.

#### 5.2 Test results with data from ICG unit connected to thorax simulator

As mentioned in the previous chapter, the waveshape of the signals when compared to the published waveforms show little correlation. The offline processing program was designed for idealized waveforms, hence the waveforms from the hardware unit with the thorax simulator do not show meaningful results.

#### 5.3 Test results with synthetic data

a) A plot of a particular sample set of data as mentioned in the previous chapter was shown in Fig 4.4. When this data was fed to the offline processing program, the display obtained at the output of the program is as shown in the Fig 5.1 and the various parameters obtained were as follows,

$$Z_o = 21.6 \Omega$$

$$HR = 100 \text{ bpm}$$

$$T_{lvet} = 0.23 \text{ sec}$$

$$SV = 41.82 \text{ ml/beat}$$

$$CO = 4.182 \text{ lpm.}$$

The display obtained as output shows the three signals, namely  $z(t)$ ,  $dz/dt$  and the ECG waveforms, can be scrolled to view the entire data file. The  $dz/dt$  waveform can be zoomed to get an enlarged view of the signal. The display also shows the ensemble averaged  $dz/dt$  signal with appropriate points marked on it.

b) The results obtained for the data with heart rate variation in step and ramp mode as explained in the last chapter are summarized below. The two values of heart

rate selected were:  $HR_l = 40$  bpm and  $HR_h = 80$  bpm. Results obtained for step mode of variation (Fig 5.2) are as follows,

$$Z_o = 21.6 \Omega$$

$$HR = 60 \text{ bpm}$$

$$T_{lvet} = 0.27 \text{ sec}$$

$$SV = 50.84 \text{ ml/beat}$$

$$CO = 3.05 \text{ lpm.}$$

Here, the value of the heart rate obtained was the average of the two values of the heart rate. The value of the stroke volume also changed since the  $dz/dt$  signal was also varied in accordance with the ECG signal.

Results obtained for ramp mode of variation (Fig 5.3) are as follows,

$$Z_o = 21.6 \Omega$$

$$HR = 49.4 \text{ bpm}$$

$$T_{lvet} = 0.28 \text{ sec}$$

$$SV = 17.09 \text{ ml/beat}$$

$$CO = 0.84 \text{ lpm.}$$

c) The results obtained for the data with stroke volume variation in step and ramp mode as explained in the last chapter are summarized below. The two values of heart rate selected were :  $SV_l = 30$  ml/beat and  $SV_h = 60$  ml/beat.

Results obtained for step mode of variation (Fig 5.4) are as follows,

$$Z_o = 21.6 \Omega$$

$$HR = 100 \text{ bpm}$$

$$T_{lvet} = 0.23 \text{ sec}$$

$$SV = 48.99 \text{ ml/beat}$$

$$CO = 4.9 \text{ lpm.}$$

Here, the heart rate does not change, only the value of stroke volume changes.

Results obtained for ramp mode of variation (Fig 5.5) are as follows,

$$Z_o = 21.6 \Omega$$

$$HR = 104 \text{ bpm}$$

$$T_{lvet} = 0.23 \text{ sec}$$

$$SV = 34.38 \text{ ml/beat}$$

$$CO = 3.6 \text{ lpm.}$$

d) Finally, all the above considered sets of data were added with white gaussian noise and the results were analyzed for varying SNRs. It was found that the

program gave satisfying results even in the presence of noise upto SNR of 15 dB. Below 15 db, no results were obtained. The display obtained with SNR of 25 db is shown in Fig 5.6. Table below shows the results for data with heart rate and stroke volume variations in the presence of noise with SNR of 25 dB.

<b>Type of signal</b>	<b>Zo (<math>\Omega</math>)</b>	<b>HR (bpm)</b>	<b>LVET (sec)</b>	<b>SV (ml/beat)</b>	<b>CO (lpm)</b>
Original data file	22.2	100	0.23	39.22	3.92
HR_STEP_40-80	22.2	60	0.27	48.13	2.89
HR_RAMP_40-80	22.2	49.4	0.28	18.84	0.93
SV_STEP_30-60	22.2	100	0.23	46.21	4.62
SV_RAMP_30-60	22.2	104	0.23	32.09	3.36

## Chapter 6

### SUMMARY AND SUGGESTIONS FOR FUTURE WORK

#### 6.1 Summary

The impedance cardiography technique is a non-invasive technique that is used to determine cardiac function from measurements of the electrical impedance of the thorax. The validity, accuracy and reliability of impedance technique rely on its correlation with other standard methods. Most of the standard methods for blood flow measurement involve catheterization and are very difficult to repeat.

The electrical models of the thorax, based on tissue resistivity and its change with blood volume, were developed in order to determine the origin of the impedance signal and the effect of blood volume changes in various regions of the thorax. The study of these models do not completely agree on the contributions of each of the various regions of the thorax, but do agree on the fact that the lungs, atria, aorta and the ventricles make significant contributions to the impedance waveform. All the models that have been developed are based on the basic assumption that the ejection of blood from the left ventricle during ventricular systole is constant, but in actual practice the ejection of blood does not remain constant. Hence the results obtained show an overestimation of the stroke volume and cardiac output.

The present work involved testing the hardware, acquisition of signals from the hardware block and analysis of acquired and synthesized data for variations in stroke volume and heart rate in the presence of noise with varying SNR values. The hardware as redesigned by Babu Kuriakose recorded the  $z(t)$ ,  $dz/dt$ ,  $Z_0$  and ECG waveforms. These signals were then interfaced to the PC with an A/D card and were further processed to obtain the various physiological parameters, namely  $Z_0$ , HR,  $T_{lvet}$ , SV and CO. The signal processing algorithm was also tested with synthesized data incorporating variations in the heart rate and stroke volume. Finally, synthesized data in the presence of noise was fed to the signal processing algorithm and was found that below SNR of 15 dB, the algorithm fails to give meaningful results.

#### 6.2 Suggestions for future work

The hardware for measurement of  $z(t)$ ,  $dz/dt$  and ECG signals will have to be modified. Balanced current source can be employed for reducing the effect of stray

magnetic fields, and improvement obtained can be studied.

The system can be incorporated with a provision of varying the excitation frequency.

The instrument can be used for recording waveforms from patients with various disorders in order to carry out investigation into modifying the signal processing algorithm, for obtaining diagnostic information and estimation of cardiac output.

The impedance measuring unit also needs to be interfaced with the notebook PC with PCMCIA based data acquisition card.

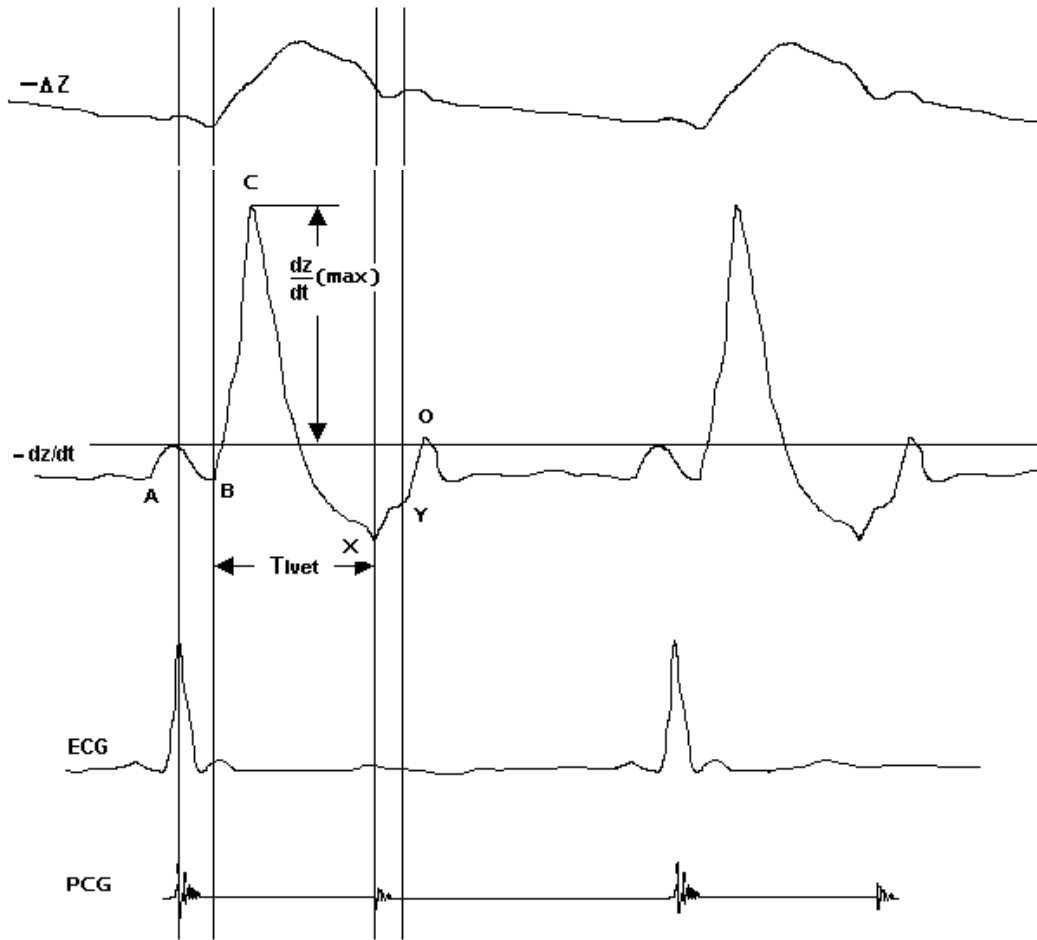


Fig. 2.1 Impedance Cardiogram (adapted from [4])

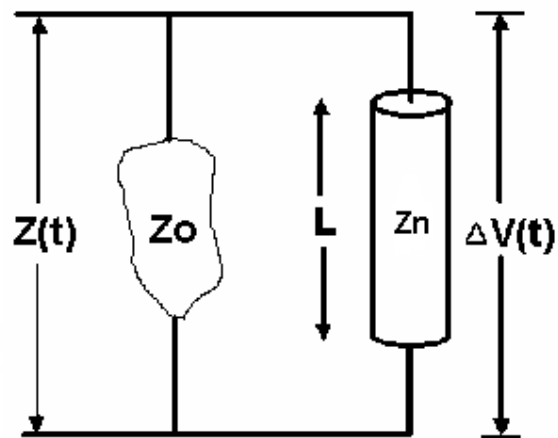


Fig. 2.2 Parallel column model (adapted from [4])

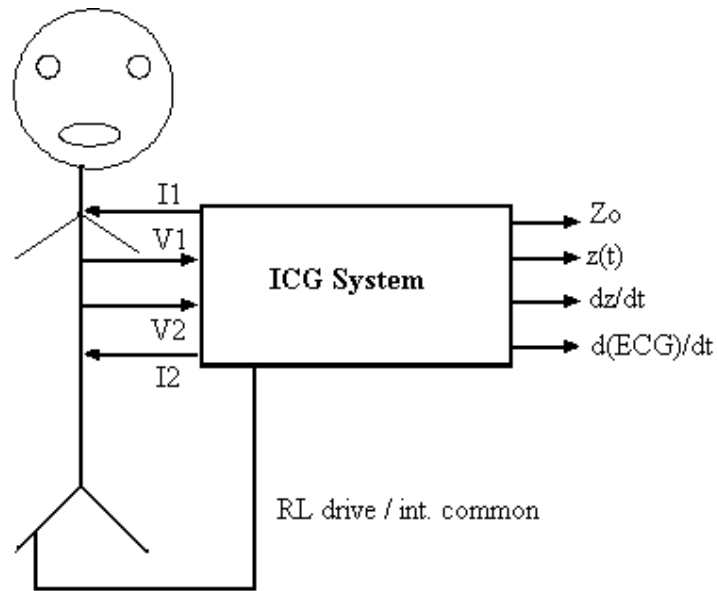


Fig 3.1 ICG system with the patient

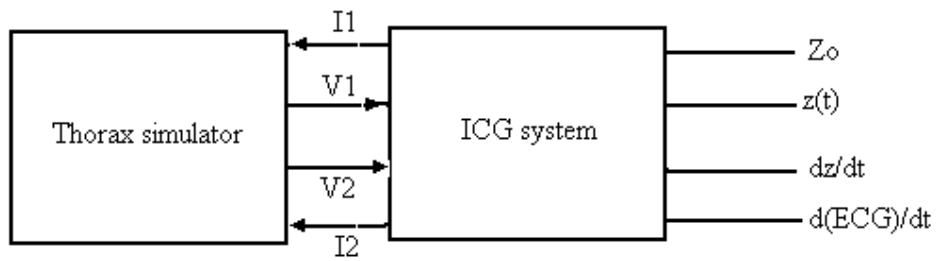


Fig 3.2 ICG system with thorax simulator

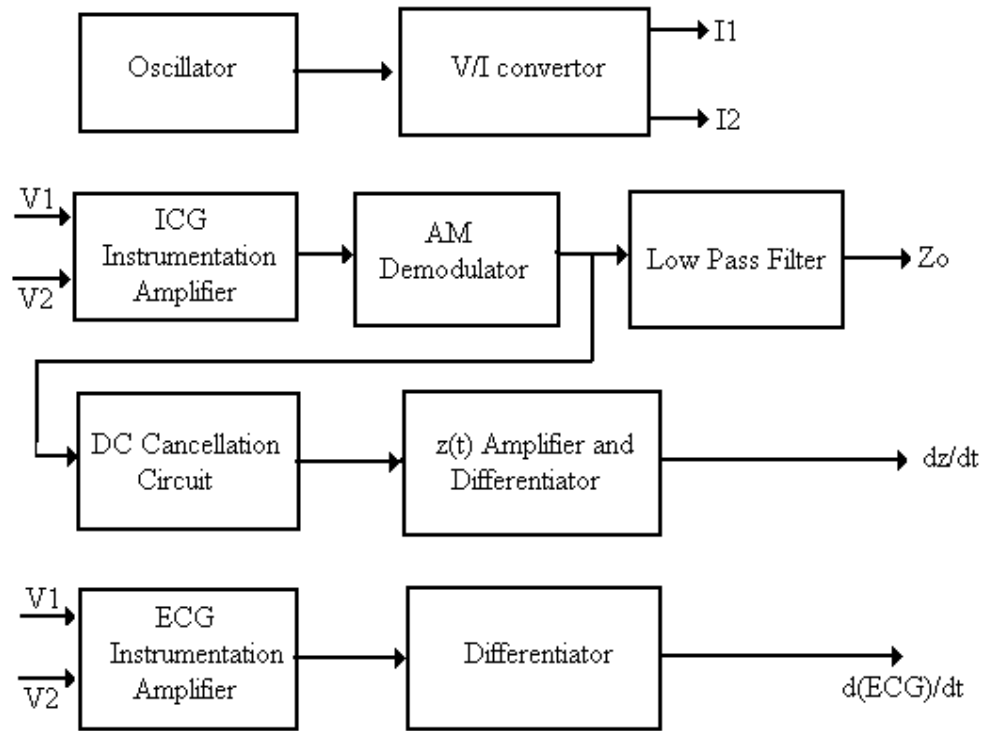


Fig 3.3 ICG system block schematic

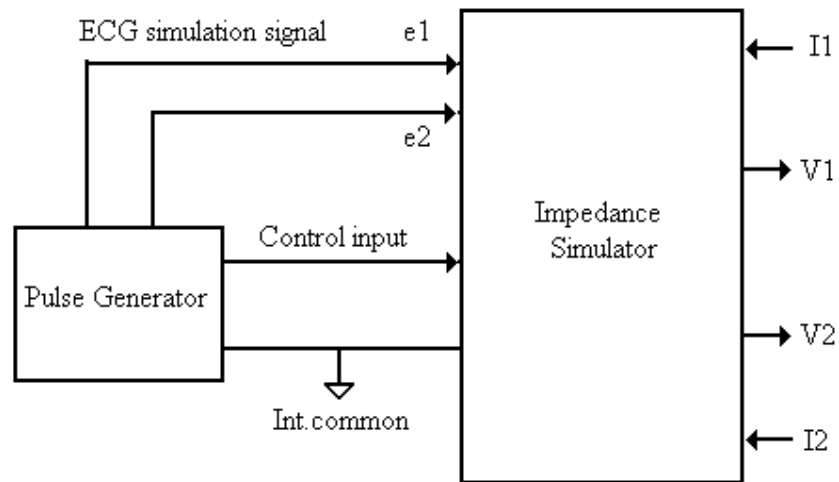


Fig 3.4 Thorax simulator block schematic

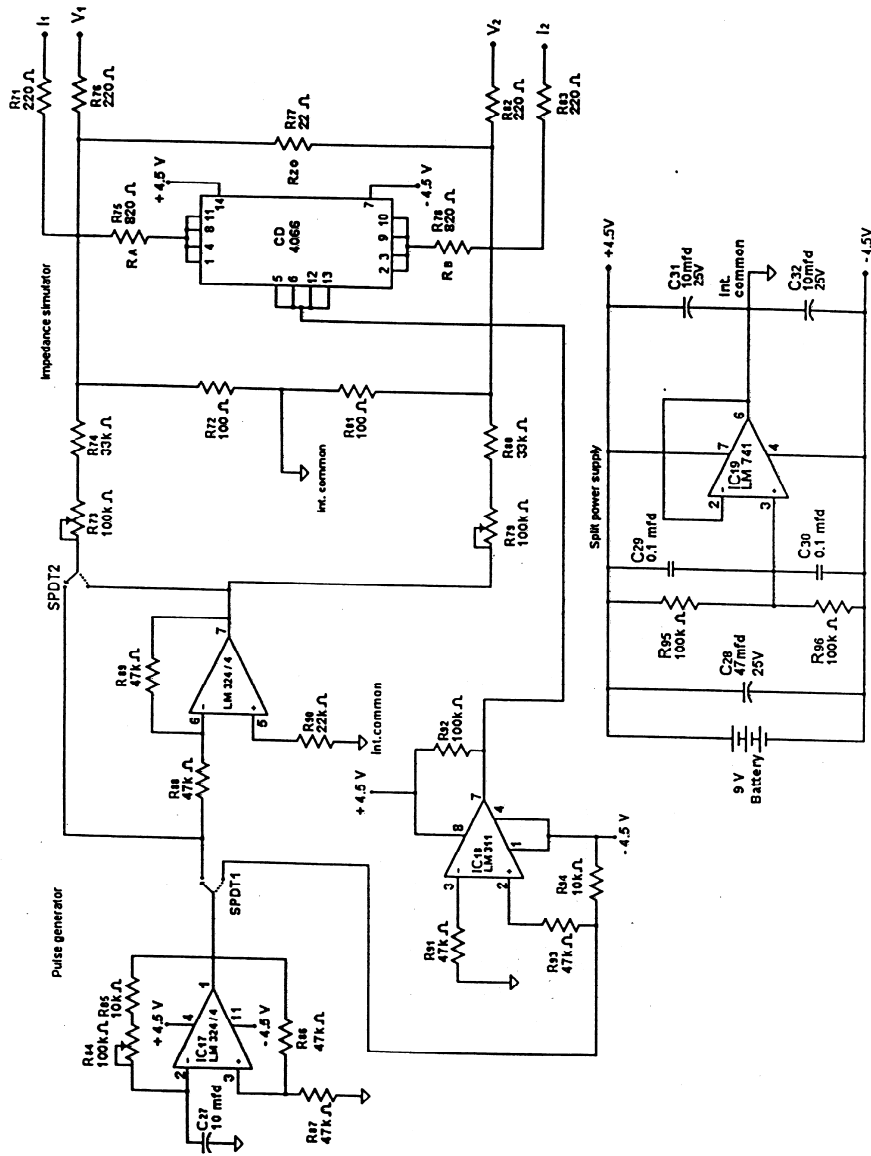


Fig 3.5 Circuit diagram of thorax simulator (adapted from [4])

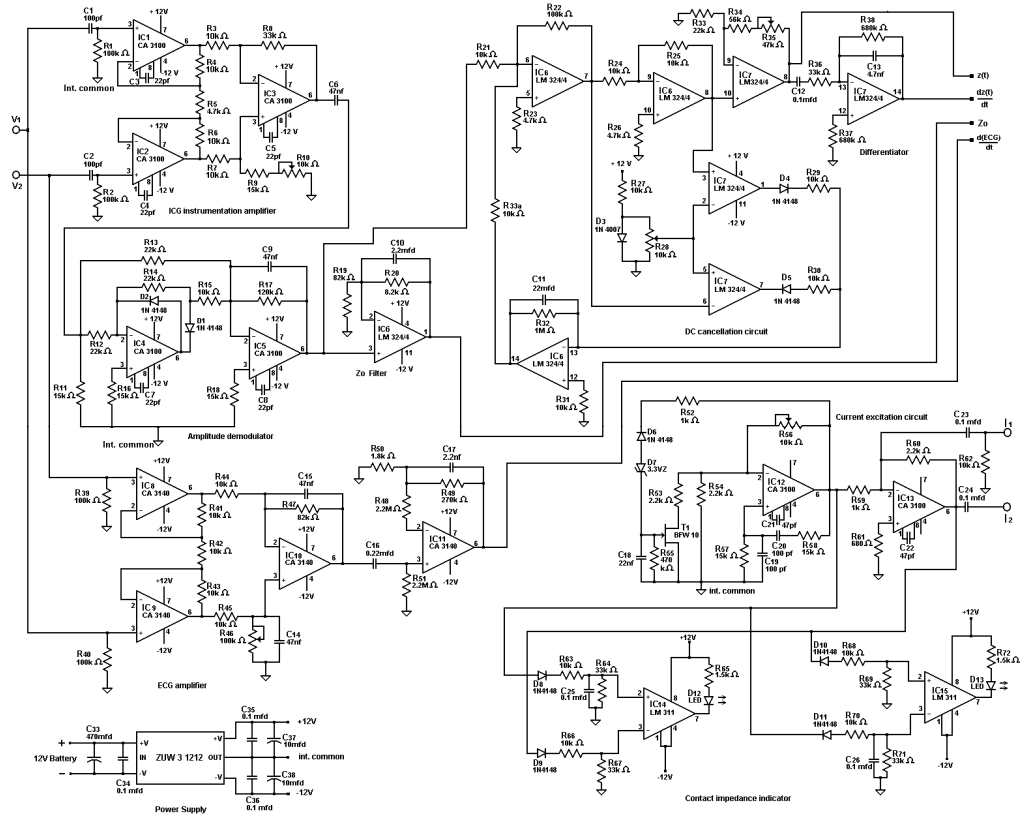


Fig B.1 Circuit schematic of ICG instrument

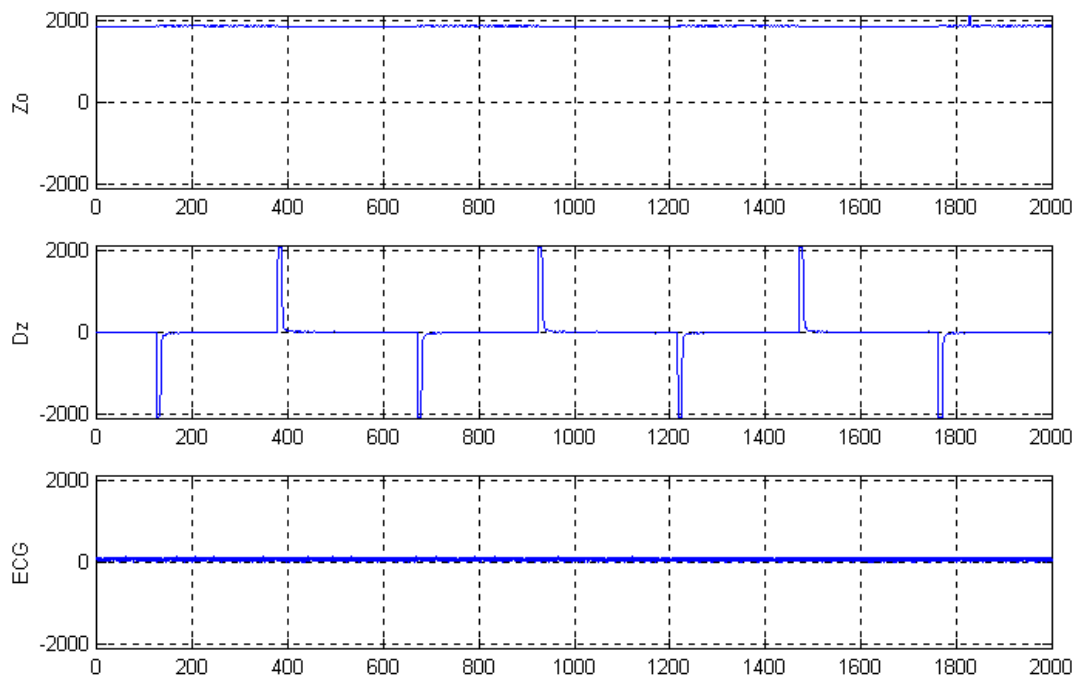


Fig. 4.1 Plot of acquired data ( $Z_0$  and  $dz/dt$ ) when thorax simulator is in ICG mode

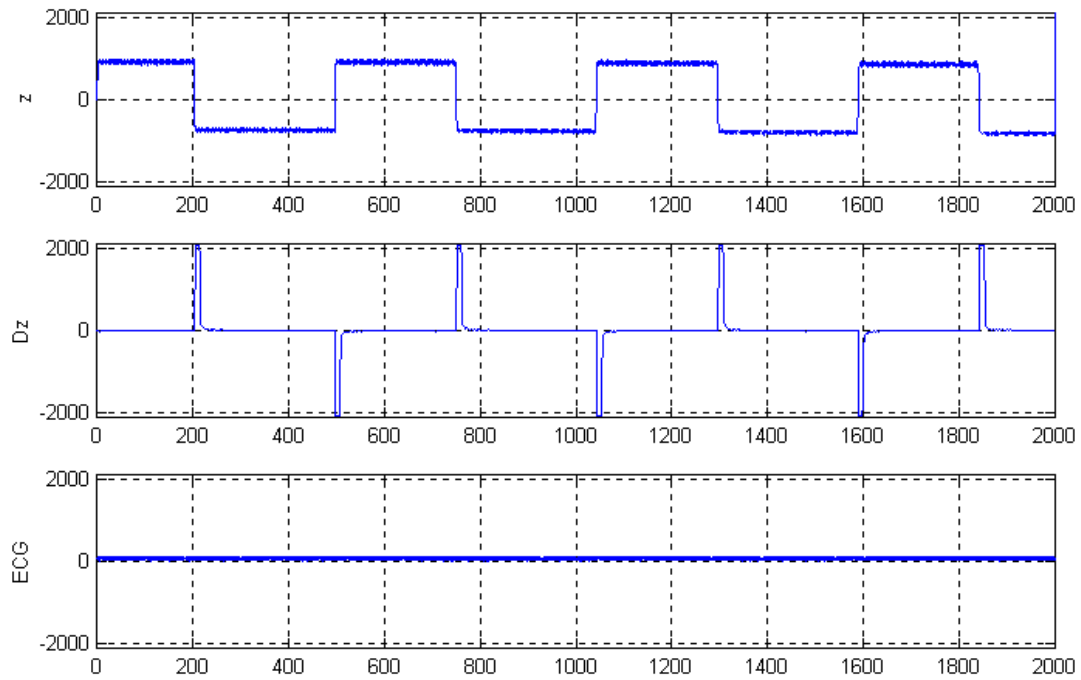


Fig. 4.2 Plot of acquired data ( $z$  and  $dz/dt$ ) when thorax simulator is in ICG mode

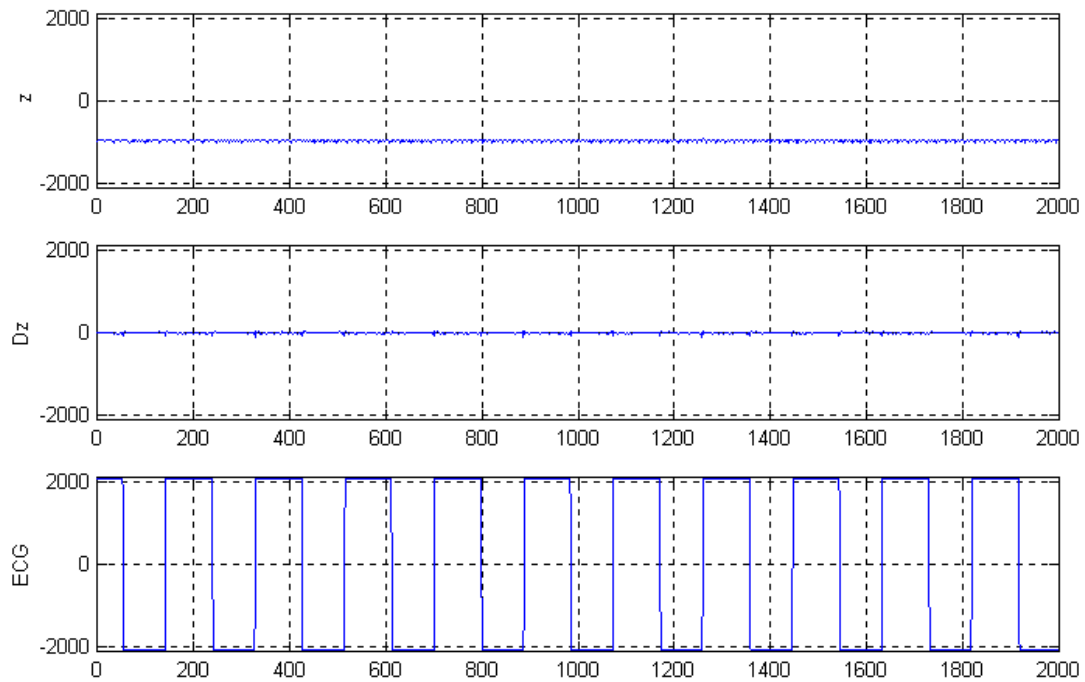


Fig. 4.3 Plot of acquired data when thorax simulator is in ECG mode

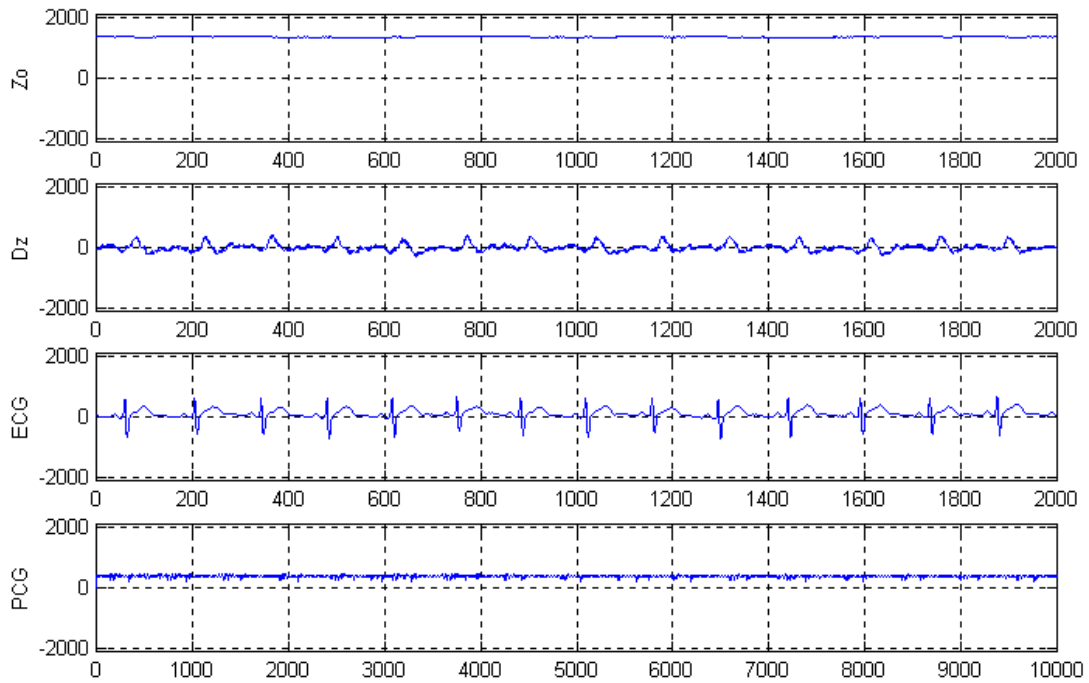


Fig. 4.4 Plot of normal synthesized data

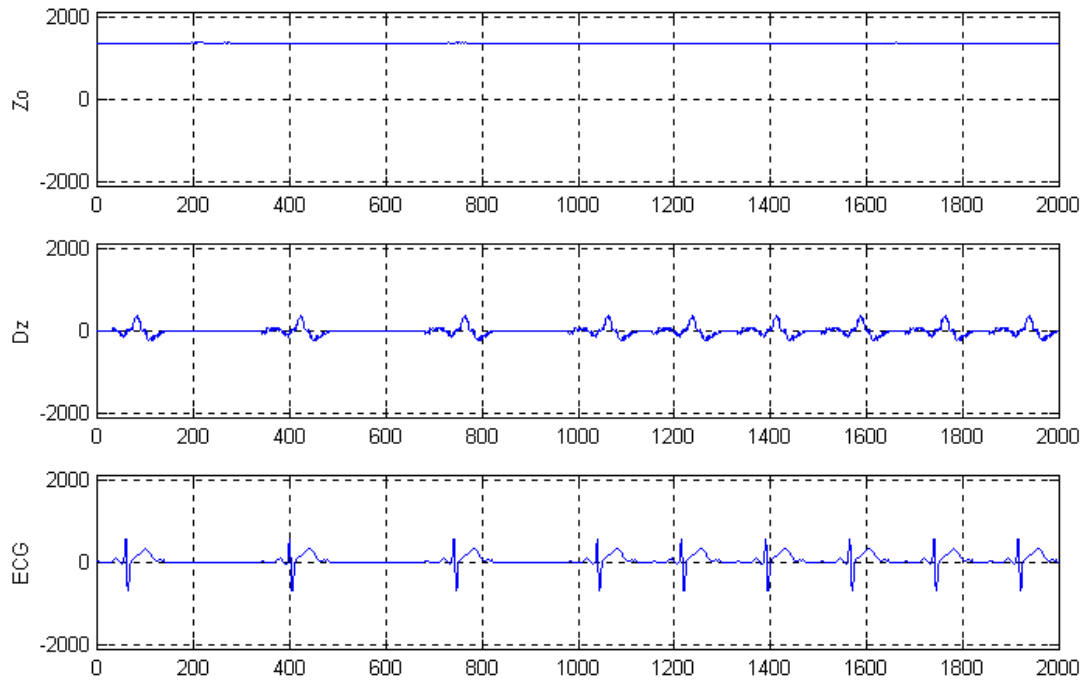


Fig. 4.5 Plot of synthesized data with heart rate variation in step mode

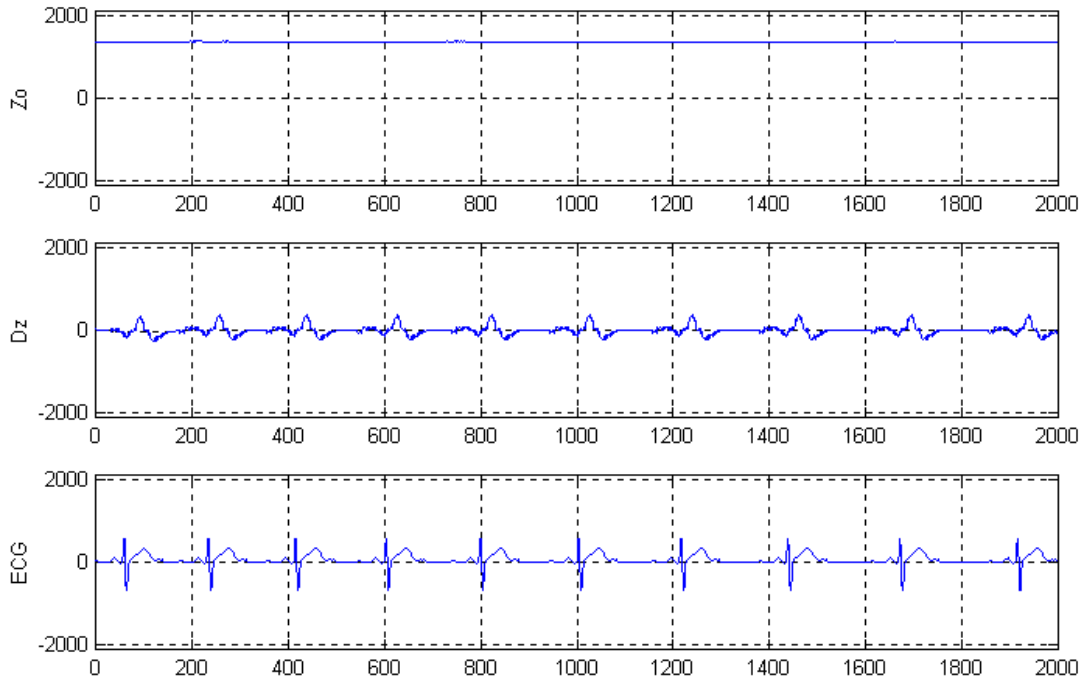


Fig 4.6 Plot of synthesized data with heart rate variation in ramp mode

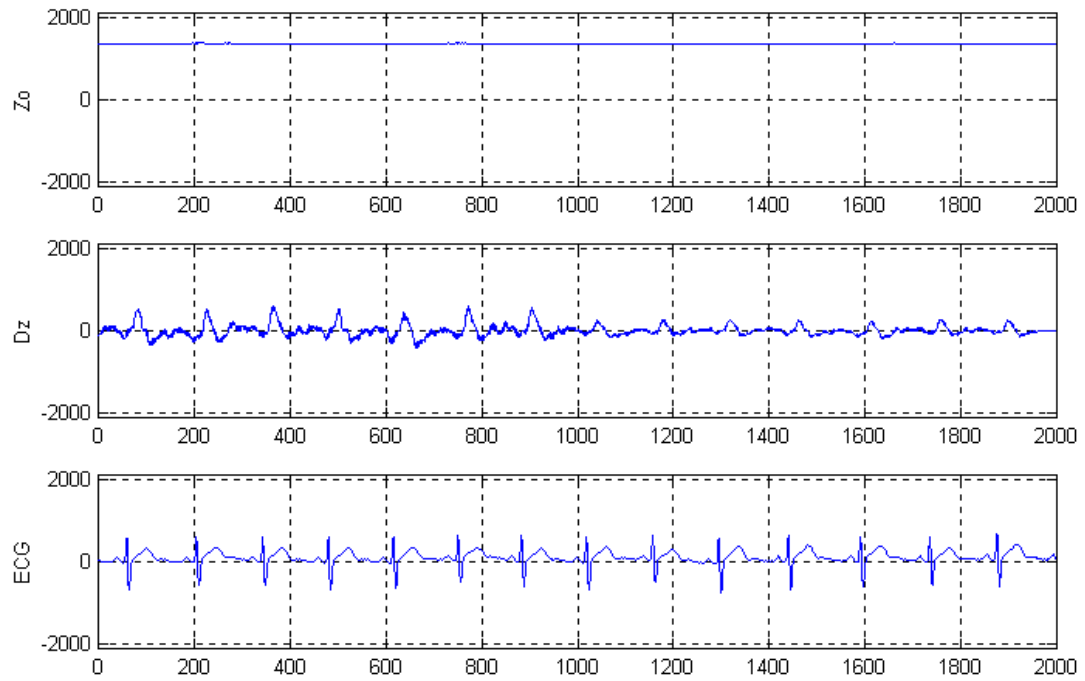


Fig. 4.7 Plot of synthesized data with stroke volume variation in step mode

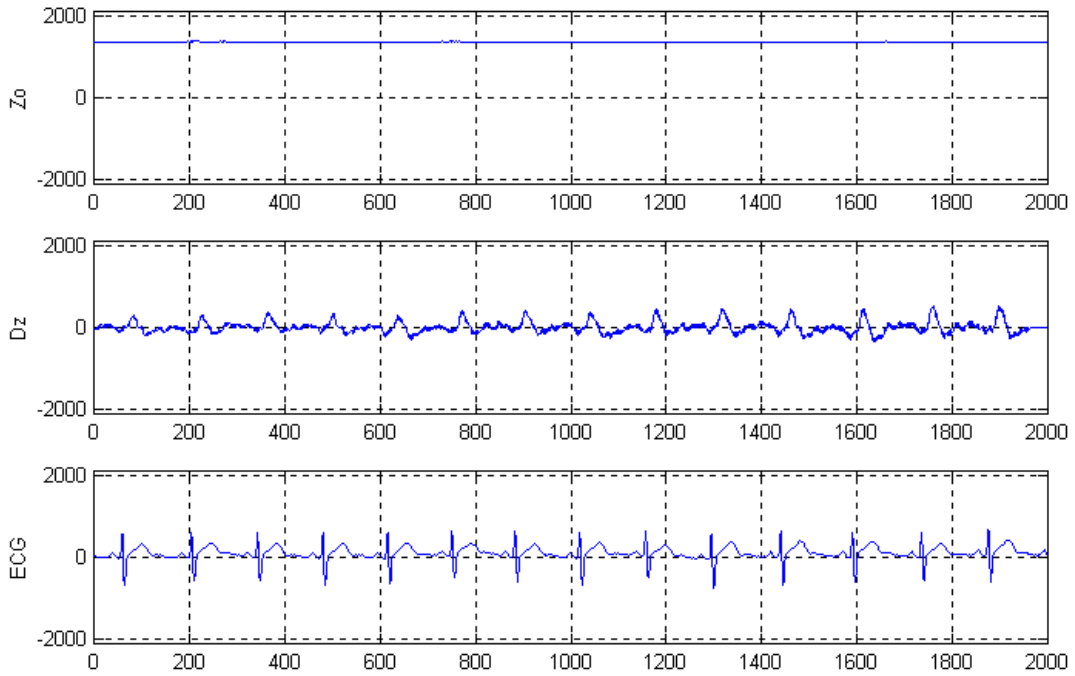


Fig. 4.8 Plot of synthesized data with stroke volume variation in ramp mode

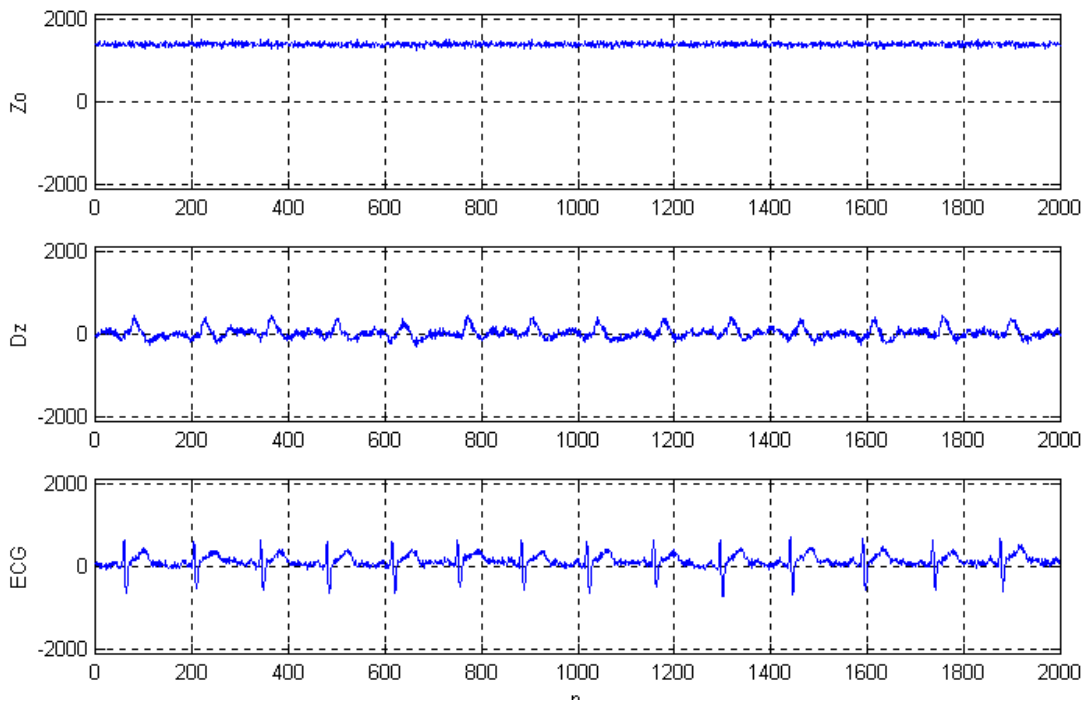


Fig. 4.9 Plot of synthesized data with white Gaussian noise (SNR=25 dB)

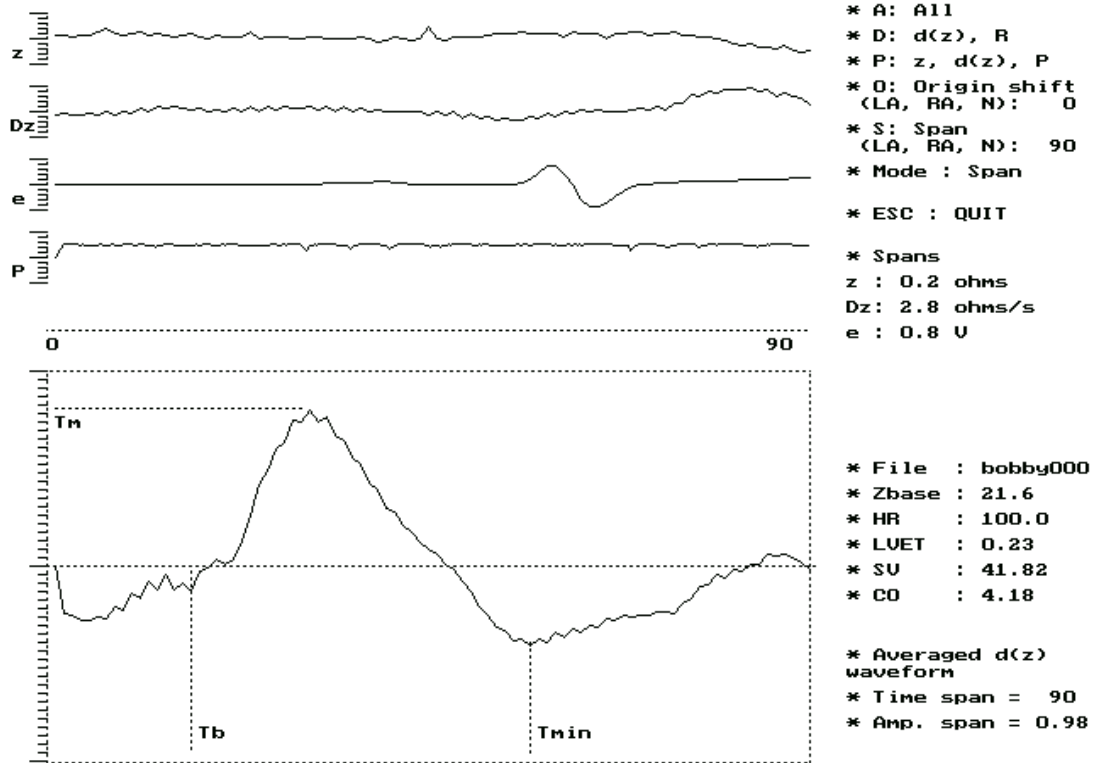


Fig 5.1 Result obtained with normal synthesized data

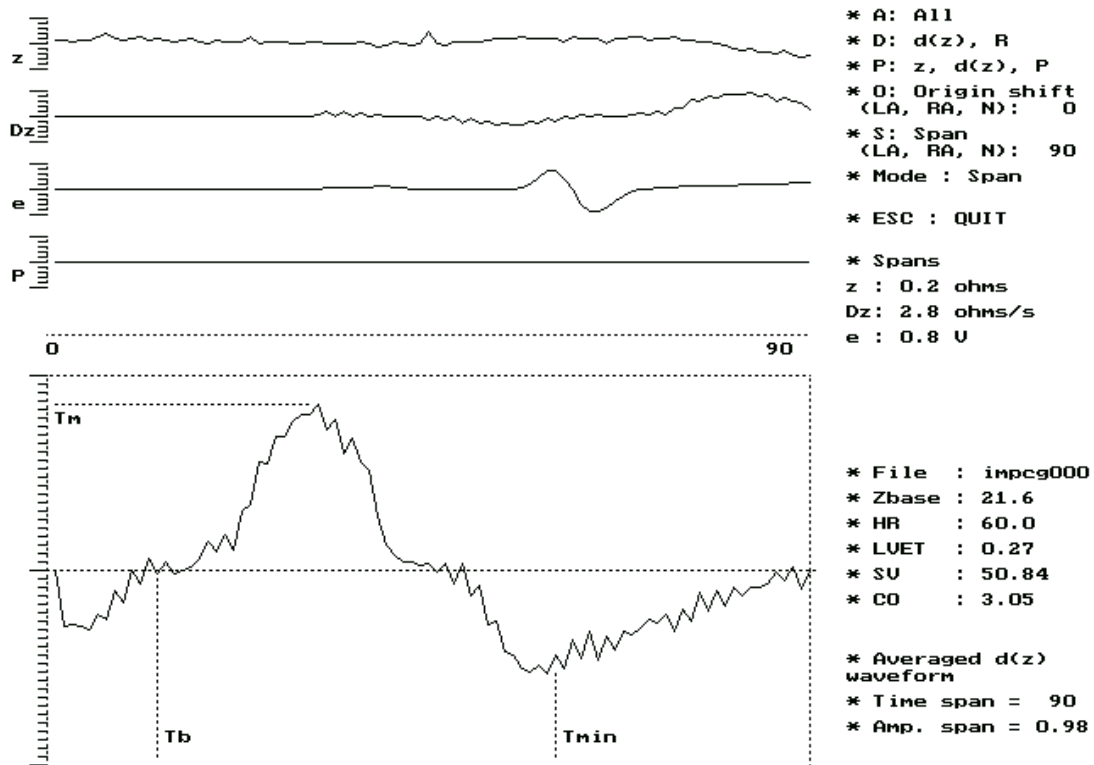


Fig 5.2 Result obtained with heart rate variation in step mode

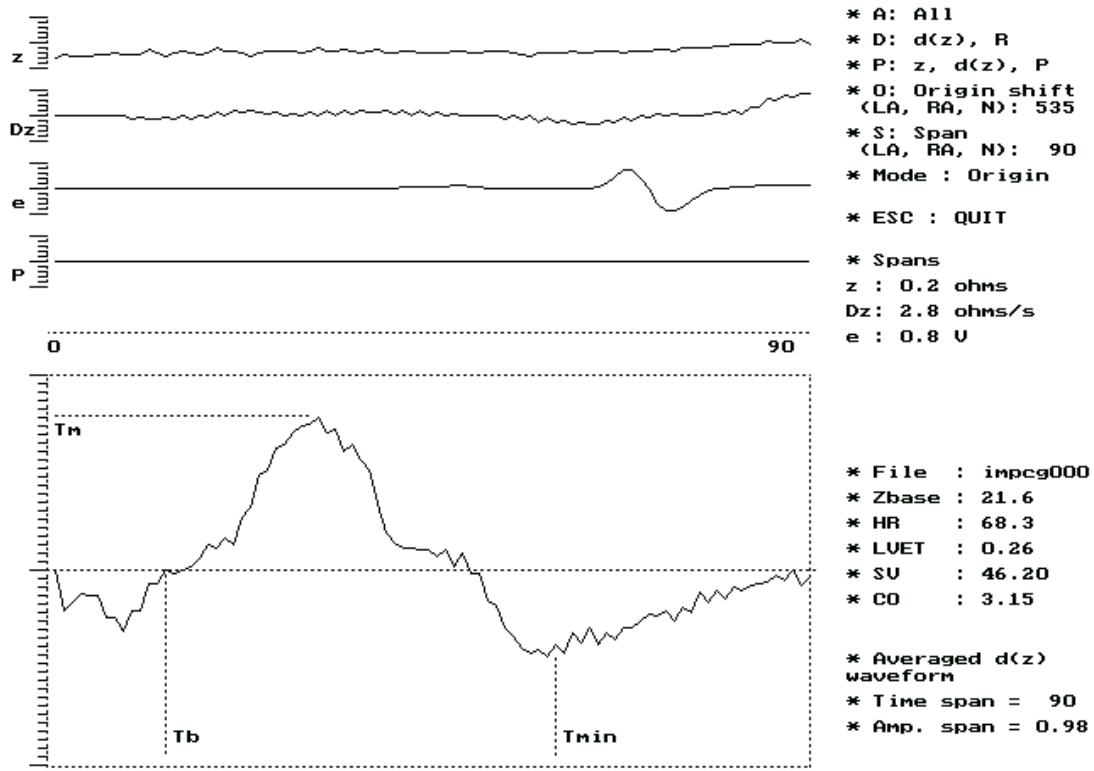


Fig 5.3 Result obtained with heart rate variation in ramp mode

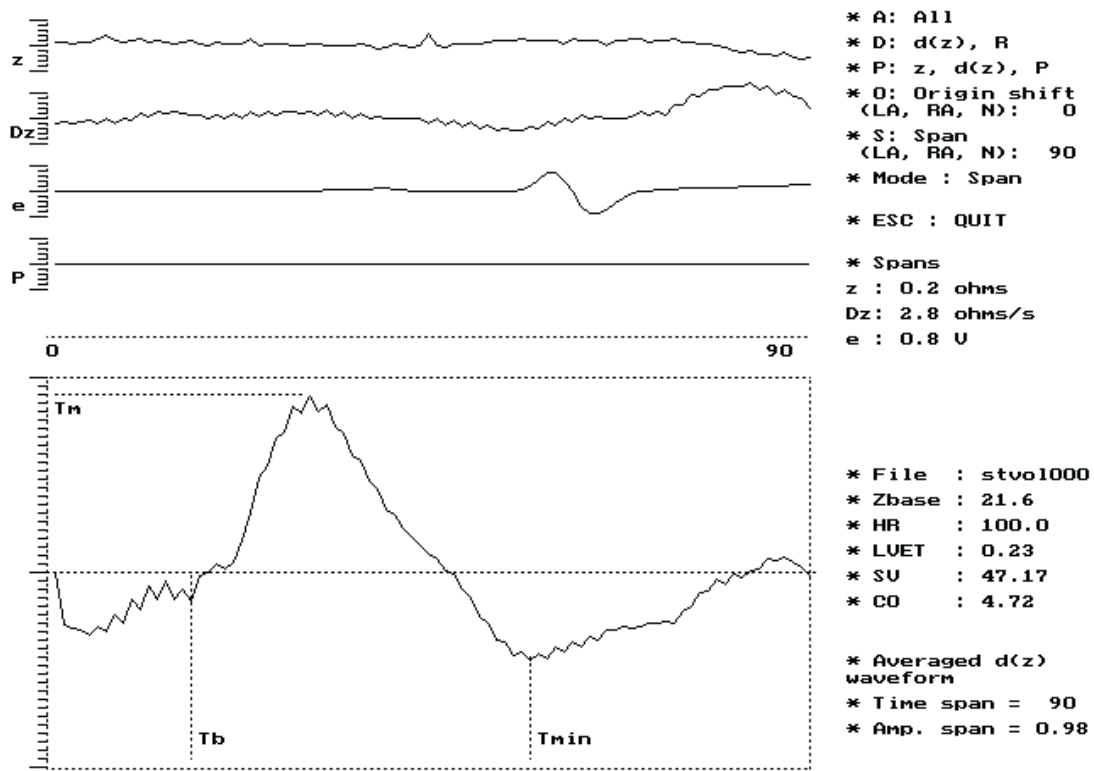


Fig 5.4 Result obtained with stroke volume variation in step mode

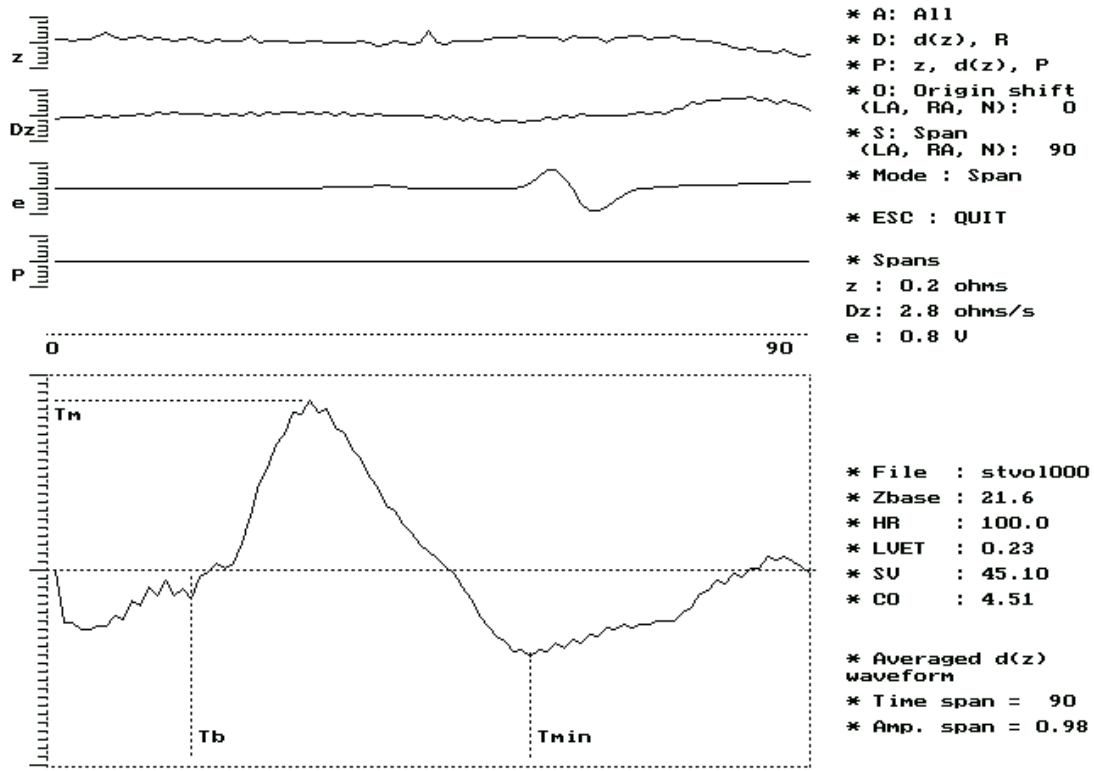


Fig 5.5 Result obtained with stroke volume variation in ramp mode

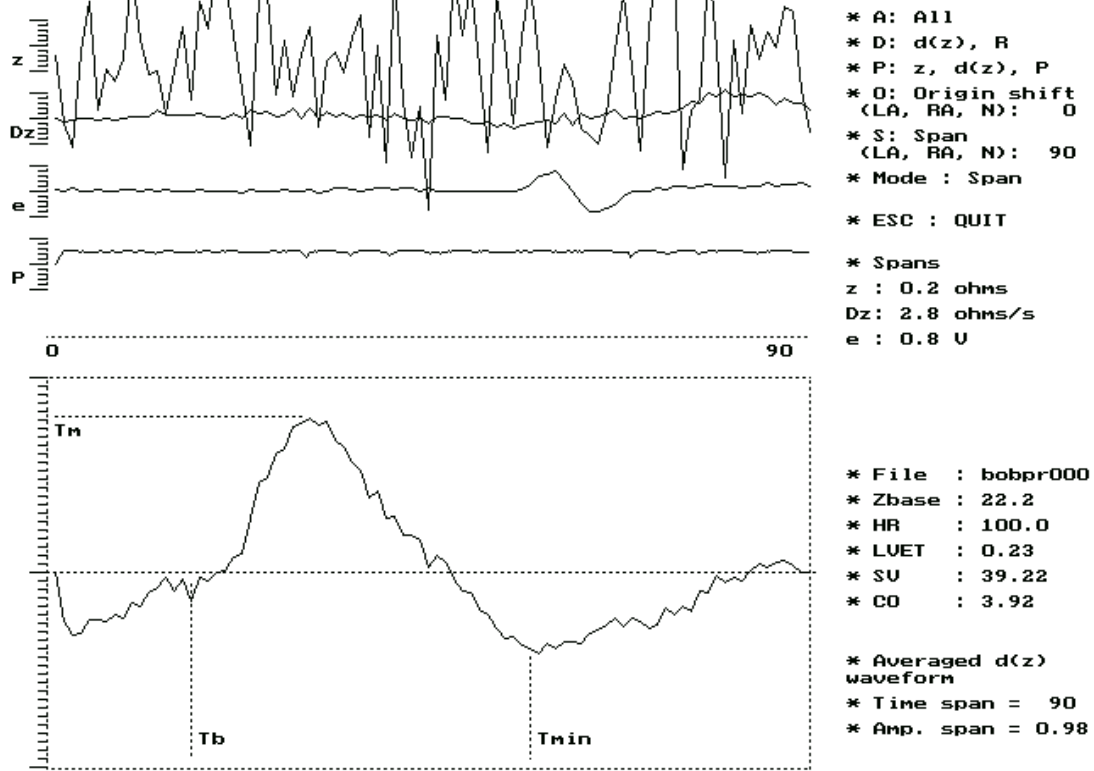


Fig 5.6 Result obtained with gaussian noise added synthesized data

## **Appendix A**

### **EARLIER SIGNAL PROCESSING SOFTWARE**

In this section, the offline signal processing software as developed by Kedar Patwardhan is described. The program SPA2B is for offline display and processing. The impedance signal  $z(t)$ , its derivative  $dz/dt$  and ECG  $e(t)$  waveforms are recorded from the hardware and stored in binary files by the signal acquisition program ICG\_ACQ. These files are then fed to the offline processing and display program for further processing.

#### **Overview**

An enhanced version for detecting QRS complex locations in the ECG has been used. Using these, the  $dz/dt$  signal is ensemble averaged. From this LVET and  $(dz/dt)_{\min}$  are found. Base impedance is found by averaging  $z(t)$ . Stroke volume is calculated using the equation derived by Kubicek. Heart rate is found from QRS complex intervals, and this, along with stroke volume for calculating cardiac output. A provision to view zoomed version of the waveforms and to process them cyclewise is also added. The following section describes the overall algorithm in detail.

#### **Signal Processing Algorithm**

The ECG signal is first processed and enhanced to get a reliable R-point detection. An enhanced version as suggested by Hamilton [8] has been used for the same.

**Step 1** : ECG signal is first low pass filtered with a cut off frequency of 11 Hz in order to remove the 50 Hz and other high frequency noise. The difference equation implementation of the filter is given as,

$$y(n) = 2y(n-1) - y(n-2) + x(n) - 2x(n-2) + x(n-12)$$

**Step 2** : This signal is then high pass filtered with a cut off frequency of 5 Hz to enhance the QRS complexes in the ECG signal. The difference equation for high pass filtering is given as,

$$y(n) = y(n-1) - x(n)/32 + x(n-16) - x(n-17) + x(n-32)/32$$

**Step 3 :** In order further enhance the QRS complex, the bandpass filtered signal is differentiated as,

$$y(n) = (2x(n) + x(n-1) - x(n-3) - 2x(n-4)) / 8$$

**Step 4 :** Finally, this signal squared and then a 32 point moving averaging filter is used to suppress all peaks of width less than that of QRS complex.

$$y(n) = \sum_{m=0}^{31} \frac{[x(n-m)]^2}{32}$$

**Step 5 :** Now, all R points are determined by a simple peak detection scheme wherein a peak is considered to be a valid QRS complex only if the amplitude of the signal exceeds a certain threshold and the width exceeds 120 msec.

**Step 6 :** Ensemble averaging of dz/dt signal is carried out from 60 sample points prior to the location of R point and it is processed to locate the maximum value in the entire dz/dt signal,  $T_{peak}$ . The baseline crossing point,  $T_{base}$  is detected as the first point prior to the  $T_{peak}$  point that has a negative value. The value of left ventricular ejection period,  $T_{lvet}$  is given as,

$$T_{lvet} = T_{min} - T_{base}$$

There is a linear relationship between heart rate and  $T_{lvet}$  given in msec as,

$$T_{lvet} = 391 - 0.91HR$$

In order to determine the value of the unknown  $T_{min}$  point, some apriori information about it is obtained by using the obtained value of  $T_{lvet}$  in the formula to calculate  $T_{min}$ . Now, a window of  $\pm 0.125(R-R)$  interval is placed around this estimated value of  $T_{min}$  and the point at which minimum value of signal in this window occurs is taken as the actual  $T_{min}$  point. Now,  $T_{lvet}$  is recalculated as,

$$T_{lvet} = T_{min} - T_{base} .$$

**Step 7** : Kubicek's modified formula is now used to calculate the SV and finally CO is calculated. The results of calculation are then displayed.

## Appendix B

### PCL-208 DATA ACQUISITION CARD SETTINGS

PCL-208 is a high performance, high speed, multifunction data acquisition card from “Dynalog Micro Systems” that can be interfaced to the PC data bus. The key features of the card used in this application are switch selectable. The various switch settings required by the signal acquisition program are now stated.

#### 1. Base address

The I/O port base address for the card is selectable via an 8 position DIP switch. The switch setting required for 300 Hex address is as shown below.

Switch position	1	2	3	4	5	6
Name	A9	A8	A7	A6	A5	A4
Setting	OFF	OFF	ON	ON	ON	ON

Here, A4.....A9 correspond to PC bus address lines.

#### 2. Channel configuration and Unipolar/Bipolar selection

Jumper SW3 and SW2 control the selection of analog input configuration and input category. Since analog signals to be digitized are all single ended and bipolar, SW3 is kept at 16 Ch position to enable 16 single-ended input channels mode and switch SW2 is appropriately positioned for Bipolar mode.

#### 3. Analog input range

The analog input range is selected by DIP switch SW1 and is kept at  $\pm 10$  V setting shown below.

Switch position	1	2	3	4	5	6
Setting	ON	OFF	OFF	OFF	OFF	OFF

#### 4. Clock frequency selection

The card offers two clock frequencies (10 MHz and 1MHz) to its internal timer/counter to generate programmable pulses to trigger the A/D. The 1 MHz clock should be selected by sliding switch SW1 to 1 MHz position.

## Appendix C

### SYSTEM SPECIFICATIONS

#### 1. Hardware

##### 1.1 ICG instrument specifications:

1. Signal conditioner

**Power source** **12 V battery, 2.5A, rechargeable**

2. Excitation circuit

Excitation frequency 100 kHz (fixed)

Excitation current 3.3 mA<sub>rms</sub>

3. Electrodes

Type Suction cup, non-polarizable

Material Stainless steel

4. Sensing circuit

The signal conditioner unit gives four outputs namely,  $z(t)$ ,  $dz/dt$ ,  $d(\text{ECG})/dt$  and  $Z_o$ .

##### 1.2 Thorax simulator specifications

1. Power requirements

D.C. source 9V rechargeable battery

Supply current 10 mA approx.

2. Electrical parameters

$\Delta R$  variation 0.2 $\Omega$  to 0.4 $\Omega$  (0.232 $\Omega$  typical)

ECG variation

- common mode 6 to 140 mV

- difference mode 2 to 30 mV

## **2. Software**

The  $z(t)$ ,  $dz/dt$  and ECG signals are digitized and stored into binary files with filesize of 12 kbytes. This is done using mains operated PC with PCL-208 data acquisition card from Dynalog Micro Systems.

The data acquired in binary files are processed by signal processing algorithm developed by Kedar Patwardhan. The signals can also be displayed and zoomed.

## REFERENCES

1. Babu Kuriakose, "An Impedance Cardiograph," *M.Tech. Dissertation*, Guide: Prof. P. C. Pandey, School of Biomedical Engg., IIT Bombay, Jan. 2000.
2. K. S. Patwardhan, "An Impedance Cardiograph for stress testing," *M.Tech. Dissertation*, Guide: Prof. P. C. Pandey, Dept. of Electrical Engg., IIT Bombay, Jan.1997.
3. G. D. Jindal, T. S. Ananthakrishnan, S. K. Kataria, and Alka Deshpande, "An introduction to impedance cardio-vasography," *BARC Report*, 2001.
4. R. P. Patterson, "Fundamentals of impedance cardiography," *IEEE Engg. in Medical and Biological Magazine*, pp. 35-38, March 1989.
5. X. Wang, H. H. Sun, and J. Water, "An advanced signal processing technique for impedance cardiography," *IEEE Trans. on Biomedical Engg.*, vol. BME-42, pp. 224-230, Feb. 1995.
6. J. Rosell and J. G. Webster, "Signal-to-motion artifact ratio versus frequency for impedance plethysmography," *IEEE Trans. on Biomedical Engg.*, vol. BME-42, pp. 321-323, March 1995.
7. "Impedance cardiography: A noninvasive way to monitor hemodynamics," <http://www.springnet.com/ce/d005a.htm>, July 1999.
8. P. S. Hamilton and W. J. Tompkins, "Quantitative investigation of QRS detection rules using the MIT/BIH arrhythmia database," *IEEE Trans. On Biomedical Engg.*, vol. BME-43, pp. 1157-1165, Dec. 1986.
9. A. J. Vander, J. H. Sherman, and D. S. Luciano, *Human Physiology*, McGraw-Hill, Third Edition, 1980.
10. R. S. Khandpur, *Handbook of Biomedical Instrumentation*, New Delhi, Tata McGraw-Hill, 1987.
11. Y. Zhang, Minghai Qu, J. G. Webster, W. Tompkins, B. Ward, and D. Bassett, "Cardiac output monitoring by impedance cardiography during treadmill exercise," *IEEE Trans. on Biomedical Engg.*, vol. BME-33, pp.1037-1041, Nov. 1986.
12. B. H. Brown, D. C. Barber, A. H. Morice, and A. D. Leathard, "Cardiac and respiratory related electrical impedance changes in the human thorax," *IEEE Trans. on Biomedical Engg.*, vol. BME-41, pp. 729-734, August 1994.

13. Manish Ingle and P. C. Pandey, "Cardiac output monitoring with an impedance cardiograph," *Conference of IEEE/EMBS and Biomedical Engg. Society of India*, pp.15-18, Feb.1995.
14. A. K. Barros, M. Yoshizawa, and Y. Yasuda, "Filtering noncorrelated noise in impedance cardiography," *IEEE Trans. on Biomedical Engg.*, vol. BME-42, pp. 324-327, March 1995.